한국화재·소방학회, 제16권 제2호, 2002년
[논 문]

T. of Korean Institute of Fire Sci. & Eng.
Vol. 16, No. 2, 2002

A Study on the Heat-Diffusion Prediction of Induction Heating JAR using Finite Element Method

유한요소법을 이용한 IH-JAR의 열확산 예측에 관한 연구

Hong-Seok Oh†

오 홍 석†

삼척대학교 소방방재공학과 겸임교수

(2002. 03. 07. 접수/2002. 05. 27. 채택)

ABSTRACT

Induction heating is widely used in today's industry, in operations such as metal hardening, pre-heating for forging operations, melting or cooking. In this paper, the magneto-thermal analysis of an induction heating jar(IH-JAR) was presented as an efficient design. The magnetic field intensity inside the axisymmetric shaped cooker was analyzed using three-dimensional axisymmetric finite element method(FLUX2D) and the effectual heat source was obtained by ohmic losses from eddy currents induced in the jar. The heat was calculated using the heat source and heating equation. Also, it was presented the temperature characteristics of the IH-JAR according to time and relative permeability in stainless parts and in aluminum parts.

요 약

유도가열 기술은 담금질, 단조를 위한 예열, 용융 그리고 요리 등과 같은 산업 전반에 걸쳐서 아주 폭넓게 사용되는 기술이다. 본 논문에서는 IH-JAR의 효과적인 설계를 위하여 자계 및 열 해석을 하였다. IH-JAR의 내부자계는 3차원 축대칭 유한요소법을 사용하여 해석하였으며, 열원은 IH-JAR 내부에서 유도된 와전류에 의하여 발생되고, 열은 열원과 열방정식을 사용하여 계산되어진다. 또한, IH-JAR의 온도분포를 시간과 투자율에 따라 제시하였다.

Keywords : Magneto-thermal, Induction Heating, Finite element method, Heat-diffusion prediction, Three-dimensional axisymmetric, IH-JAR

1. Introduction

Induction heating describes the thermal conductivity problem in which the heat is generated by ohmic losses from eddy currents induced in conducting media, such as stainless steel and aluminum, by a varying magnetic field.[1,2] Recently, induction heating jar (IH-JAR) is very interesting for high efficiency, the low heating time and the convenient regulation of heating spot. The magnetic field intensity and the heat source in the IH-JAR should be exactly calculated in order to make uniform temperature distribution required on the surface of the IH-JAR. But, the waste of time and cost has been increased because the design method of the IH-JAR in the industry is depending on the experience. Therefore, it is continuously required that the development of precision design method is based on the exact magnetic field intensity and heat source.[3-7] In this paper, the magneto-thermal analysis of the IH-JAR was presented as an efficient design. And the magnetic field intensity inside the axisymmetric shaped cooker was analyzed using three-dimensional axisymmetric finite element method (FLUX2D), and

† E-mail: ohhong@dreamwiz.com

the effective heat source was obtained by the calculation of the induction current in the IH-JAR. The heat-diffusion prediction was calculated using the heat source and heating equation.

2. The Eddy Current Problem

The construction of the IH-JAR can be applied to the three-dimensional axisymmetric finite element method because it has the same form for circular direction. The governing equation of the eddy currents problem is described by the following equation (1). Here we assume that the sources of the magnetic field have sinusoidal time dependence.

$$\frac{1}{\mu}\nabla\times\nabla\times A + j\omega\sigma A = J_0 \tag{1}$$

where A is the magnetic vector potential, μ is the permeability of mass, σ is the electric conductivity of mass, J_0 is the sinusoidal exciting current density and ω represents the angular frequency of the sinusoidal exciting current. The finite element equation can be expressed with the standard Galerkin's method, the vector equations and the boundary condition's as follow:

$$\int_v \frac{1}{\mu}(\nabla\times W_i\cdot\nabla\times A)dv + \int_v j\omega\sigma W_i\cdot A dv = \int_v J_0\cdot W_i dv \tag{2}$$

where W_i is the weight function. The current density, the magnetic vector potential and the weight function can be expressed with the cylindrical coordinate system as shown by equation (3) because of three-dimensional axisymmetric problem.

$$J_0 = J_0\theta,\ A = A\theta,\ W_i = W_i\theta \tag{3}$$

Substituting equation (2) into equation (3), we obtain equation (4).

$$\frac{\pi}{\mu}\int\left(\frac{1}{r^2}\frac{\partial(rA)}{\partial z}\frac{\partial(rW_i)}{\partial z}+\frac{1}{r^2}\frac{\partial(rA)}{\partial r}\frac{\partial(rW_i)}{\partial r}\right)drdz + 2\pi j\omega\sigma\int W_i A drdz = 2\pi\int J_0 W_i rdrdz \tag{4}$$

Substituting $A_R = rA$ and $N_i = rW_i$ into the equation (4), we get for the finite element equation as follows:

$$\int\frac{1}{\mu r}\left(\frac{\partial A_R}{\partial z}\frac{\partial N_i}{\partial z}+\frac{\partial A_R}{\partial r}\frac{\partial N_i}{\partial r}\right)drdz + j\omega\sigma\int\frac{1}{r}N_i A_R drdz = \int J_0 N_i drdz \tag{5}$$

where A_R is the state variable and N_i is the shape functions. To make the element matrix, the shape functions in the triangular element can be approximated as the equation (6).

$$N_i = \frac{b_i + c_i r + d_i z}{2\Delta^e} \tag{6}$$

where Δ^e is the area of the triangular element. And the state variable in the triangular element can be expressed by the equation (7) with the help of equation (6)

$$A_R^e = \sum_{j=1}^{3} N_j A_{Rj} \tag{7}$$

where A_{Rj} is the state variable values in the each node of the triangular element.

Substituting equation (5) into equation (6) and (7), we can obtain the element matrix equation (8) with the equations (9) and (10).

$$K^e A^e = f^e \tag{8}$$

$$K_{ij}^e = \frac{1}{4\mu\Delta^e r_0}(c_i c_j + d_i d_j) + j\frac{\omega\sigma\Delta^e}{3r_0}(1+\delta_{ij}) \tag{9}$$

$$f_i^e = \frac{J_0\Delta^e}{3} \tag{10}$$

where δ_{ij} is the Kronecker-Delta.

The system matrix equation (11) can be obtained by applying equation (8) to every element.

$$[K][A] = [f] \tag{11}$$

where [K] is the coefficient matrix and [f] is the driving vector.

It can be calculated the magnetic vector potential, the eddy current and the heat source in each node by solving the system matrix equation. And the eddy current, J_e, is the equation (12) from ohms law as

shown below.

$$J_e = \sigma E_e = -\sigma\frac{\partial A}{\partial t} = -j\omega\sigma A \quad (12)$$

where $\partial A/\partial t$ is vector potential to time.

The heat source per unit volume, ht_s, is written as equation (13).

$$ht_s = \frac{|J_e|^2}{\sigma} = \omega^2\sigma|A|^2 = \omega^2\sigma AA^* \quad (13)$$

3. The FE-model of the IH-JAR

Figure 1 and table 1 are respectively the three-dimensional axisymmetric FE-model of the IH-JAR and the material constants of it. Figs. 2 and 3 are respectively the flux lines of case 1($\mu_r = 1$) and of case 2($\mu_r = 100$). Here we know that the flux lines cannot completely pass through the inner IH-JAR because of the skin effect of the stainless steel.

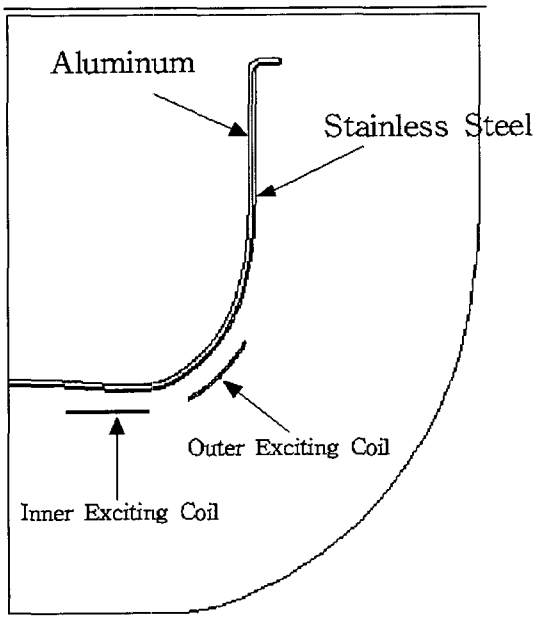

Fig. 1. The FE-model of the IH-JAR.

Table 1. The material constants of the IH-JAR

	Stainless Steel	Aluminum
Relative permeability(μ_r)	1(case 1) 100(case 2)	0.25×10^{-7}
Electric conductivity(s)	1.66667×10^6	4.0×10^7
Thermal conductivity(k)	30	204

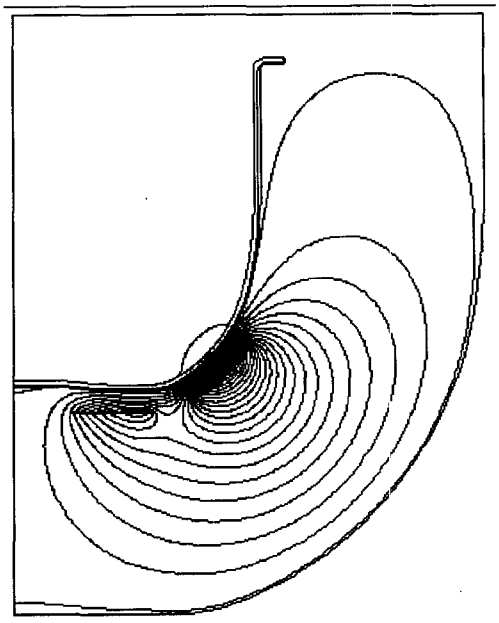

Fig. 2. The flux lines of the IH-JAR (μr = 1).

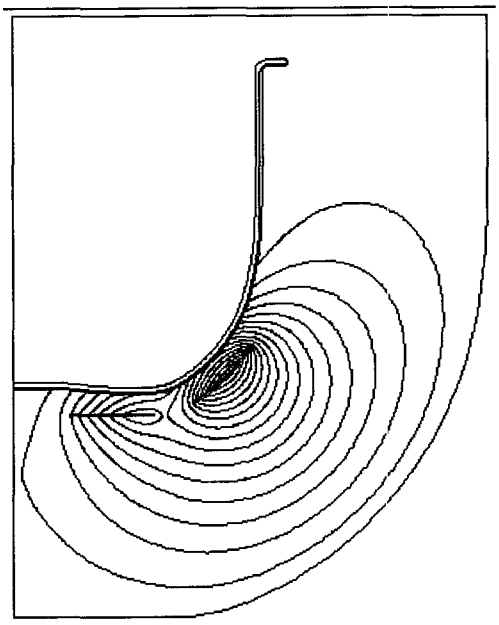

Fig. 3. The flux lines of the IH-JAR (μr = 100).

4. The FE-equations for the Heat Analysis of the IH-JAR

The three-dimensional axisymmetric heat conduction equation in the steady state is expressed as follow:

$$\frac{1}{r}\frac{\partial}{\partial r}\left(kr\frac{\partial T}{\partial r}\right)+\frac{\partial}{\partial z}\left(k\frac{\partial T}{\partial z}\right)=-ht_s \tag{14}$$

where ht_s is the heat sources and k is the thermal conductivity. The complex boundary condition between the surface of the IH-JAR and the area around it is described by equation (15).

$$-k\frac{\partial T}{\partial n}=h(T-T_\infty) \tag{15}$$

where h is the convective exchange coefficient, T is the temperature in the boundary surfaces, T_∞ is the temperature of the fluid and $\partial T/\partial n$ is the normal component of the temperature in boundary surfaces. Arranging equation (14), we obtain equation (16).

$$-\frac{\partial}{\partial r}\left(r\frac{\partial T}{\partial r}\right)-\frac{\partial}{\partial z}\left(r\frac{\partial T}{\partial z}\right)=r\frac{ht_s}{k} \tag{16}$$

The heat conduction equation can be obtained with the standard Galerkin's method as follows.

$$\iint_A\left\{r\left(\frac{\partial T}{\partial r}\right)^2+r\left(\frac{\partial T}{\partial z}\right)^2\right\}2\pi r\,dr\,dz = \iint_A 2Tr\left(\frac{ht_s}{k}\right)2\pi r\,dr\,dz \tag{17}$$

And the element matrix can be expressed by the equations (18), (19) and (20).

$$K^eT^e=f^e \tag{18}$$

$$K_{ij}^e=\frac{\pi}{2\Delta^e}r_0^2(c_ic_j+d_id_j) \tag{19}$$

$$f_i^e=\frac{\pi r_0\Delta^e ht_s}{6}\frac{ht_s}{k}(2r_i+r_j+r_k) \tag{20}$$

where r_0 is $(r_1+r_2+r_3)/3$.

Also, the element matrix equation in the complex boundary is expressed as follows:

$$[K^e+\overline{K^e}]T^e=[f^e+\overline{f^e}] \tag{21}$$

where,

$$\overline{K^e}=\int_{A_2^e}\sigma N^{et}N^e dS \tag{22}$$

$$\overline{f^e}=\int_{A_2^e}gN^{et}dS \tag{23}$$

where σ is h/k, g is hT_∞/k and A_2^e is the elements on the boundary with the complex boundary condition.

If σ is constant inside an element and the opposite side of node i-th is the complex boundary surface, the equations (22) and (23) can be respectively expressed in terms of equations (24) and (25).

$$[\overline{K^e}]_i=\frac{\pi\sigma(c_i^2+d_i^2)^{1/2}}{6}\times\begin{bmatrix}3r_k+r_j & 0 & r_k+r_j\\ 0 & 0 & 0\\ r_k+r_j & 0 & r_k+3r_j\end{bmatrix} \tag{24}$$

$$[\overline{f^e}]_i=\frac{\pi g(c_i^2+d_i^2)^{1/2}}{3}\begin{bmatrix}2r_k+r_j\\ 0\\ r_k+2r_j\end{bmatrix} \tag{25}$$

Substituting equation (21) into equations (24) and (25), we can obtain the element matrix with the complex boundary condition. If the system matrix is constructed using the above equations and it is solved, the temperature in each node can be obtained.

5. The Results of Heat-Diffused Prediction

5.1 Case 1(μ_r=1)

Fig. 4 is shown the temperature curve of the inner surface of it in 5 second. Here we know that the temperature of the IH-JAR near the outer exciting coil is maximum and the temperature of it near the inner

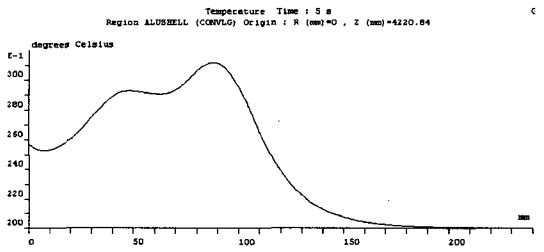

Fig. 4. The temperature curve of the IH-JAR (5 sec).

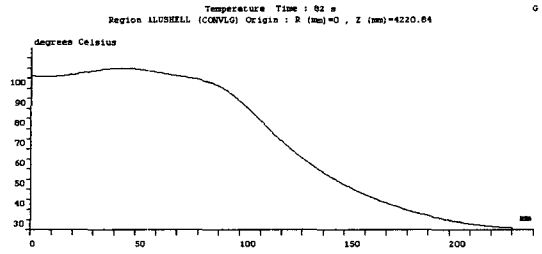

Fig. 5. The temperature curve of the IH-JAR (82 sec).

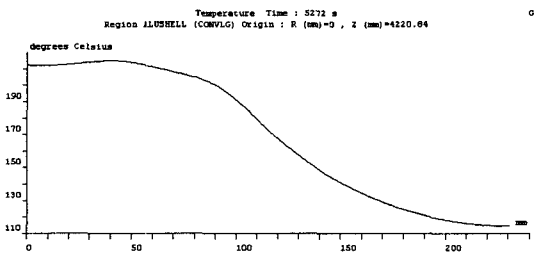

Fig. 6. The temperature curve of the IH-JAR (final time).

exciting coil is the next value. The temperature of aluminum is higher than that of stainless steel at point distant from the heat source because the thermal conductivity of aluminum is larger than that of stainless steel.

Fig. 5 is shown the temperature curve of the inner surface of it in 82 second.

Fig. 6 is shown the temperature curve of the inner surface of it in the final time.

5.2 Case 2(μ_r=100)

Fig. 7 is shown the temperature curve of the inner surface of it in 5 second.

Fig. 8 is shown the temperature curve of the inner surface of it in 56 second.

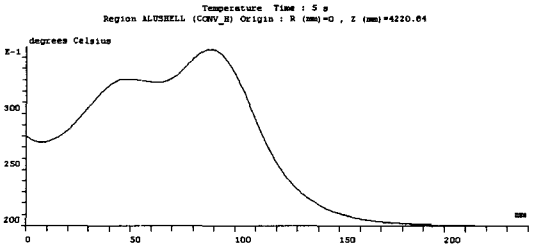

Fig. 7. The temperature curve of the IH-JAR (5 sec).

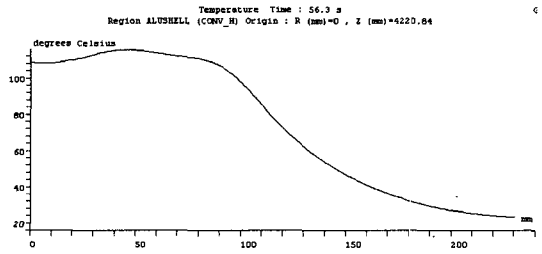

Fig. 8. The temperature curve of the IH-JAR (56 sec).

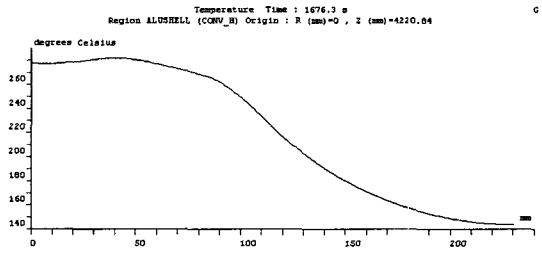

Fig. 9. The temperature curve of the IH-JAR (final time).

Fig. 9 is shown the temperature curve of the inner surface of it in the final time.

Here we know that the temperature of the IH-JAR is rapidly reached its peak as the value of relative permeability is high.

5.3 The temperature characteristics

Figs. 10 and 11 is shown respectively the temperature characteristics of the IH-JAR according to time and relative permeability in stainless steel parts and in aluminum parts.

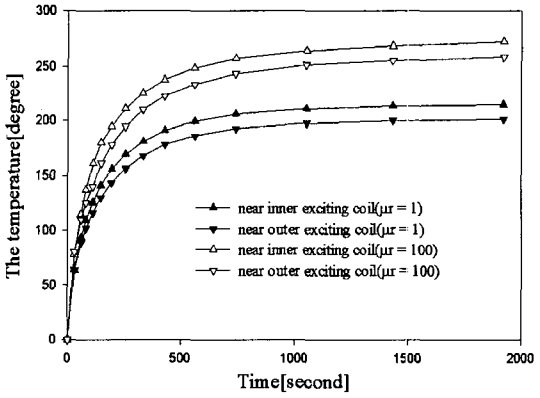

Fig. 10. The temperature curve of the IH-JAR according to time and relative permeability in stainless steel.

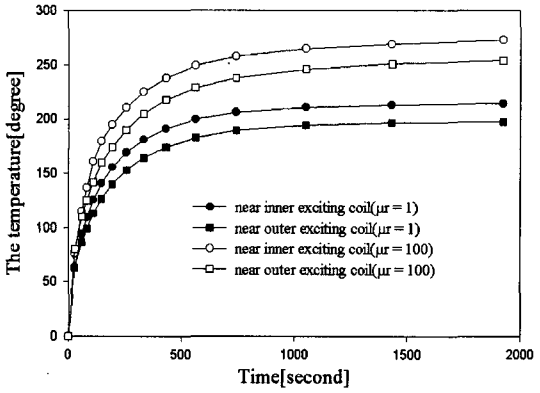

Fig. 11. The temperature curve of the IH-JAR according to time and relative permeability in aluminum.

Here we know that the temperature of the IH-JAR near the outer exciting coil is larger than that at its near inner exciting coil at the initial time, and the temperature of it near the inner exciting coil is maximum at final time.

The temperature of aluminum is higher than that of stainless steel at point distant from the heat source because the thermal conductivity of aluminum is larger than that of stainless steel. Also we know that the temperature of the IH-JAR is rapidly reached its peak value as the value of relative permeability is high.

6. Conclusions

In this paper, the magneto-thermal analysis of the IH-JAR was presented as an efficient design. And the magnetic field intensity inside the axisymmetric shaped cooker was analyzed using three-dimensional axisymmetric finite element method (FLUX2D), and the effectual heat source was obtained by the calculation of the induction current in the IH-JAR. The temperature of the IH-JAR near the outer exciting coil is larger than that at near the inner exciting coil at the initial time, and the temperature near the inner exciting coil is maximum at final time. The temperature of aluminum is higher than that of stainless steel at point distant from the heat source because the thermal conductivity of aluminum is larger than that of stainless steel. The temperature of the IH-JAR rapidly reaches its peak value as the value of relative permeability is high.

References

1. Tatsuya FURUKAWA, Itsuya MUTA and Tatsuhiko KOSUGI, "Finite Element Analysis of Induction Heating Range", Reports of the Faculty of Science and Engineering, Saga University, pp. 81-87(1988).
2. Piotr Urbanek, Adam Skork, "Magnetic Flux and Temperature Analysis in Induction Heated Steel Cylinder", IEEE Trans. on Mag., Vol. 30, No. 5, pp.3328-3330(1994).
3. L. Gong, R. Hagel, and R. Unbehauen, "On the 3-D Inhomogeneous Induction Heating of a Shell", IEEE Trans. on Mag., Vol.30, No.5, pp.3324-3327, 1994.
4. Tanroku Miyoshi, Munehiko Sumiya, and Hideki Omori, "Analysis of an Induction Heating System by Finite Element Method", T.IEE Japan, RM-86-53, pp.117-125(1986).
5. H.H.J.M. Janssen, E.J.W. ter Maten, D.van Houwelingen, "Simulation of Coupled Electro-magnetic and Heat Dissipation Problems", IEEE Trans. on Mag., Vol. 30, No. 5, pp.3331-3334(1994).
6. Zs. Badics, H. Riedler, and H. Stogner, "Application of FEM to Coupled Electric Thermal and Mechanical Problems", IEEE Trans. on Mag., Vol. 30, No. 5, pp.3316-3319(1994).
7. Hong-Seok Oh, "A Study on the Heat-Diffused Prediction of Induction Heating JAR using Finite Element Method", International conference IEB, pp.234-240(2002).